

SPATIAL DOMAIN IMAGE ENHANCEMENT AND RESTORATION TECHNIQUES

¹ KINITA B VANDARA, ² DR. G.R.KULKARNI

¹ Research Scholar, Department of Electronics and Communication Engineering,
Shri J.J.T.University, Vidyanagari, Jhunjhunu, Rajasthan

² Principal, C.U.Shah College Of Engineering And Technology, Wadhwan - 363030
Gujarat

kinitawandra.er@gmail.com, grkulkarni29264@rediffmail.com

ABSTRACT : The aim of medical image enhancement and restoration is to effectively extract information contained in the image for diagnosis. This paper discusses the standard techniques of image enhancement and restoration for medical images. Experimental results of Ultrasonography (USG) modalities are presented and analysed.

1. Introduction

Image enhancement is the processing of images to improve their appearance to human viewers, in terms of better contrast and visibility of features of interest, or to enhance their performance in subsequent computer-aided analysis and diagnosis. The objective of medical image enhancement is dependent on the application context and is often poorly defined, and the criteria are often subjective, image enhancement techniques be appropriate to be ad hoc. Image enhancement is basically improving the interpretability or perception of information in images for human viewers and providing 'better' input for other automated image processing techniques.

Image restoration concerns the removal or reduction of degradations that have occurred during the acquirement of the image. Such degradations may include noise, which are errors in pixels values, or optical effects such as out of focus blurring due to sensor motion.

2. Image Enhancement

The principal objective of enhancement is to process an image so that the result is more suitable than the original image for a specific application. The word specific is important, because it establishes at the outset that the techniques discussed in this paper are very much problem oriented. Thus, for example, a method that is quite useful for enhancing Ultrasound images may not necessarily be the best approach for enhancing pictures of Mars transmitted by a space probe. Regardless of the method used, however, image enhancement is one of the most interesting and visually appealing areas of image processing.

Image enhancement approaches fall into two categories: i) spatial domain methods ii) frequency domain methods. The term spatial domain refers to the image plane itself, and approaches in this category are based on direct manipulation of pixels in an image. Frequency domain processing procedures are based on reforming the Fourier transform of an image. Enhancement techniques based on various combinations of methods from these two categories are not unusual. We note also that many of the fundamental techniques introduced in this paper in the context of enhancement are used in subsequent papers for a variety of other image processing applications.

There is no general theory of image enhancement. When an image is processed for visual interpretation, the viewer is the ultimate judge of how well a particular method works. Visual evaluation of image quality is a highly subjective process, thus making the definition of a "good image" an elusive standard by which to compare algorithm performance. When the problem is one of processing images for machine perception, the evaluation task is somewhat easier. For example, in dealing with a character recognition application, and leaving aside other issues such as computational requirements, the best image processing method would be the one yielding the best machine recognition results. However, even in situations when a clear-cut criterion of performance can be imposed on the problem, a certain amount of trial and error usually is required before a particular image enhancement approach is selected.

In spatial domain techniques, we directly deal with the image pixels. The pixel values are manipulated to achieve desired enhancement. In frequency domain methods, the image is first transferred in to frequency

domain. It means that, the Fourier Transform of the image is computed first. All the enhancement operations are performed on the Fourier transform of the image and then the Inverse Fourier transform is performed to get the resultant image. These enhancement operations are performed in order to modify the image brightness, contrast or the distribution of the grey levels. As a consequence the pixel value (intensities) of the output image will be modified according to the transformation function applied on the input values.

Image enhancement is applied in every field where images are ought to be understood and analyzed. For example, medical image analysis, analysis of images from satellites etc. Image enhancement simply means, transforming an image f into image g using T . (Where T is the transformation. The values of pixels in images f and g are denoted by r and s , respectively. As said, the pixel values r and s are related by the expression,

$$s = T(r) \quad \dots 1$$

Where, T is a transformation that maps a pixel value (r) into a pixel value (s). The results of this transformation are mapped into the grey scale range as we are dealing here only with grey scale digital images. So, the results are mapped back into the range $[0, L-1]$, where $L=2^k$, k being the number of bits in the image being considered. So, for instance, for an 8-bit image the range of pixel values will be $[0, 255]$.

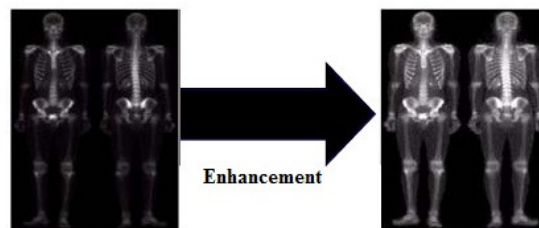


Figure 1 the Effect of Image Enhancement

2.1 Point Processing Operation

The simplest spatial domain operations occur when the neighbourhood is simply the pixel itself. In this case T is referred to as a grey level transformation function or a point processing operation. Point processing operations takes the formation shown in equation (1).

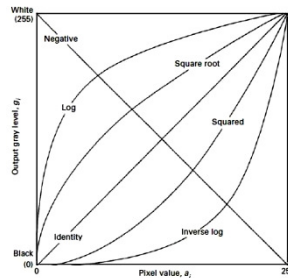


Figure 2 Basic grey level transformations

i. Image Negatives

The most basic and simple operation in digital image processing is to compute the negative of an image. The negative of an image with gray levels in the range $[0, L-1]$ is obtained by using the negative transformation shown in Figure 2, which is given by the expression

$$s = L - 1 - r \quad \dots 2$$

Reversing the intensity levels of an image in this manner produces the equivalent of a photographic negative. This type of processing is particularly suited for enhancing white or gray detail embedded in dark regions of an image, especially when the black areas are prevailing in size. The pixel gray values are inverted to compute the negative of an image. For example, if an image of size $R \times C$, having maximum gray value 255, where R represents number of rows and C represents number of columns, is represented by $I(r, c)$. The negative $N(r, c)$ of image $I(r, c)$ can be computed as

$$N(r, c) = 255 - I(r, c) \text{ where } 0 \leq r \leq R \text{ and } 0 \leq c \leq C \quad \dots 3$$

The resultant image becomes negative of the original image. Negative images are useful for enhancing white or grey detail embedded in dark regions of an image.

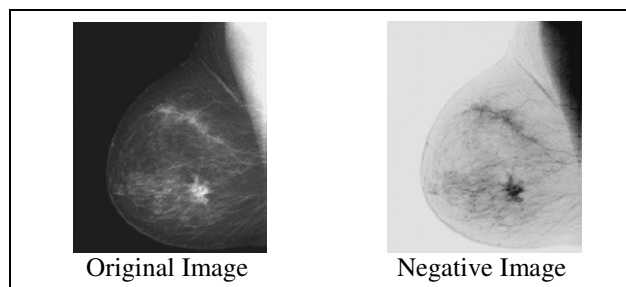


Figure3 Original digital mammogram and Negative image obtained using the negative transformation using equation 3

ii. Thresholding in spatial domain Transformations

Thresholding transformations are particularly useful for segmentation in which we want to isolate an object of interest from a background as shown in figure below.

$$s = \begin{cases} 1 & r > \text{threshold} \\ 0 & r \leq \text{threshold} \end{cases} \quad \dots 4$$

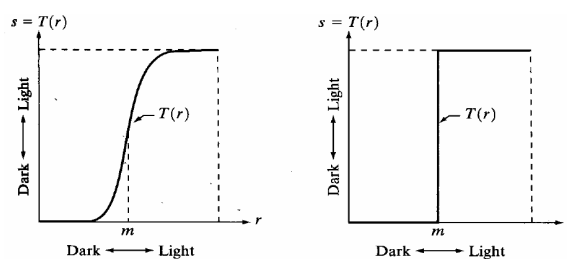


Figure 4 Thresholding transfer function

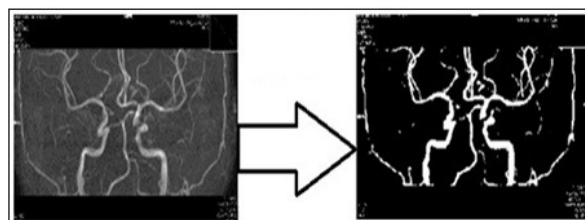


Figure 5 Thresholding transformation applied on Angiography MR Image

iii. Logarithmic Transformations

The general form of the log transformation is

$$s = c * \log(1 + r) \quad \dots 5$$

The log transformation maps a narrow range of low input grey level values into a wider range of output values. The inverse log transformation performs the opposite transformation. Log functions are particularly useful when the input grey level values may have an extremely large range of values. In the following example the Fourier transform of an image is put through a log transform to reveal more detail.

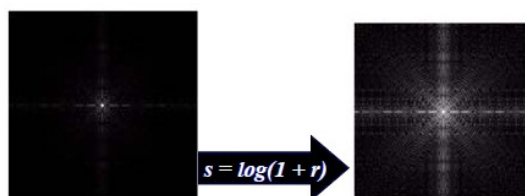


Figure 6 Effect of Logarithmic Transformation

iv. Powers-Law Transformations

The n th power and n th root curves shown in fig. A can be given by the expression,

$$s = cr^\gamma$$

This transformation function is also called as gamma correction. For various values of γ different levels of enhancements can be obtained. This technique is quite commonly called as Gamma Correction. If you notice, different display monitors display images at different intensities and clarity. That means, every monitor has built-in gamma correction in it with certain gamma ranges and so a good monitor automatically corrects all the images displayed on it for the best contrast to give user the best experience. The difference between the log transformation function and the power-law functions is that using the power-law function a family of possible transformation curves can be obtained just by varying the λ . These are the three basic image enhancement functions for grey scale images that can be applied easily for any type of image for better contrast and highlighting. Using the image negation formula given above, it is not necessary for the results to be mapped into the grey scale range $[0, L-1]$. Output of $L-1-r$ automatically falls in the range of $[0, L-1]$. But for the Log and Power-Law transformations resulting values are often quite distinctive, depending upon control parameters like λ and logarithmic scales. So the results of these values should be mapped back to the grey scale range to get a meaningful output image. For example, Log function $s = c \log (1 + r)$ results in 0 and 2.41 for r varying between 0 and 255, keeping $c=1$. So, the range $[0, 2.41]$ should be mapped to $[0, L-1]$ for getting a meaningful image.

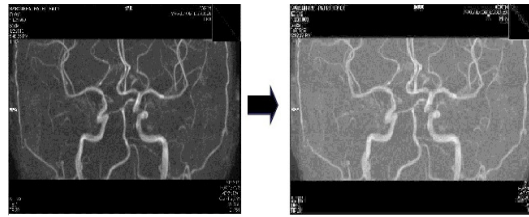


Figure 7 Power Law Transformations

V. Histogram Processing

The histogram of a digital image with intensity levels in the range $[0, L-1]$ is a discrete function

$$h(r_k) = n_k \quad \dots 6$$

r_k = k th intensity value

n_k = number of pixels in the image with intensity r_k

Histograms are frequently normalized by the total number of pixels in the image, assuming an $M \times N$ image, a normalized histogram.

$$p(r_k) = \frac{n_k}{MN}, \quad k = 0, 1, 2, \dots, L-1 \quad \dots 7$$

Is related to probability of occurrence of r_k in the image

- *Histogram Equalization*

Histogram equalization is a common technique for enhancing the appearance of images. Presume we have an image which is mostly dark. Then its histogram would be skewed towards the lower end of the grey scale and the entire image feature is solid into the dark end of the histogram. If we could 'stretch out' the grey levels at the dark end to produce a more uniformly distributed histogram then the image would become much clearer.

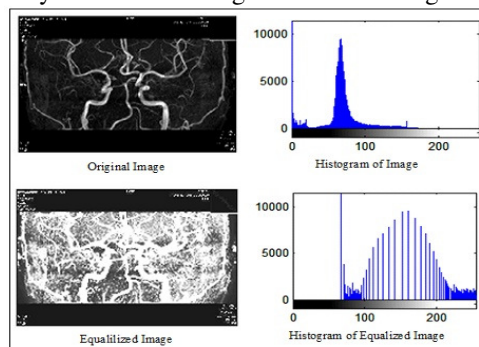


Fig. 8 Histogram Equalization of Angiography MR Image

- *Histogram Matching*

Histogram equalization automatically determines a transformation function seeking to produce an output image with a uniform histogram. Another method is to generate an image having a specified histogram is histogram matching.

1. Find the histogram $p_r(r)$ of the input image and determine its equalization transformation.

$$s = T(r) = (L-1) \int_0^r p_r(w) dw \quad \dots 8$$

2. Use the specified PDF $p_z(r)$ of the output image to obtain the transformation function:

$$G(z) = (L - 1) \int_0^z p_z(t) dt = s \quad \dots 9$$

3. Find the inverse transformation $z = G^{-1}(s)$ the mapping from s to z :

$$z = G^{-1}[T(r)] = G^{-1}(s) \quad \dots 10$$

Obtain the output image by equalizing the input image first; then for each pixel in the equalized image, perform the inverse mapping to obtain the corresponding pixel of the output image. Histogram matching enables us to “match” the gray scale distribution in one image to the gray scale distribution in another image.

2.2 Results of Basic Image Enhancement Techniques

Basic Image enhancement techniques performed on various images of Ultrasonography modality and their results are given below.

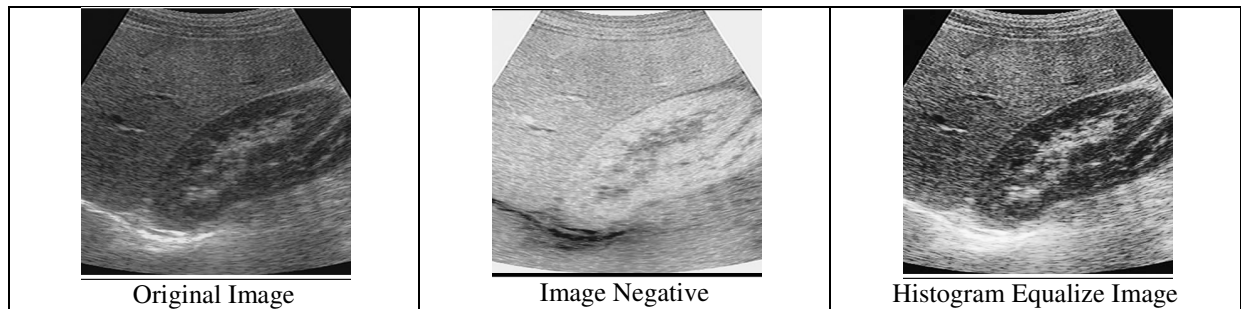


Figure 9 Results of basic Enhancement technique for USG Kidney Image

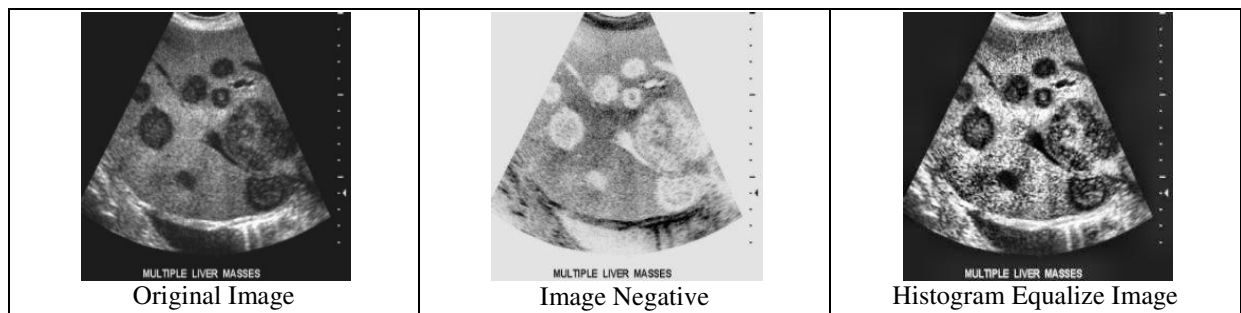


Figure 10 Results of basic Enhancement technique for USG focal liver image

3. Image Restoration

The concept of image restoration differs significantly from the idea of image enhancement. While enhancement aims at improving the appearance of the image or its properties with respect to the following analysis (by a human operator or even automatic), the goal of restoration is to remove an identified distortion from the observed image, thus providing the best possible estimate of the original undistorted image. The observed image may be distorted by blur, geometrical deformation and non linear contrast transfer.

3.1 A Model Of Image Degradation

The process of image degradation and restoration can be described by the model which is shown in figure 11. Where $f(x, y)$ represents an original image and $g(x, y)$ is the corrupted image. In the model, $n(x, y)$ represents an additive noise introduced by the system, and $h(x, y)$ is the point spread function of the blur, while $f'(x, y)$ and $p(x, y)$ are restored image and restoration system purpose, respectively. The degraded image can be modelled by:

$$g(x, y) = f(x, y) * h(x, y) + n(x, y) \quad \dots 11$$

Where, * stands for convolution. Due to processing the image in digital form, the above equation can be written in the matrix-vector form. The expression of the equation in frequency domain by the Fourier Transform is

$$G(u, v) = F(u, v) H(u, v) + N(u, v) \quad \dots 12$$

So, if we design a restoration filter:

$$P(u, v) = \frac{1}{H(u, v)}$$

$$F'(u, v) = \frac{F(u, v) H(u, v)}{H(u, v)} + \frac{N(u, v)}{H(u, v)} \quad \dots 13$$

Given the degraded image $g(x, y)$, if we can estimate the $h(x, y)$, namely PSF, the restored image will be obtain. Based on this theory, it is crucial to identify the true PSF, a very difficult task for the limitation of prior knowledge.

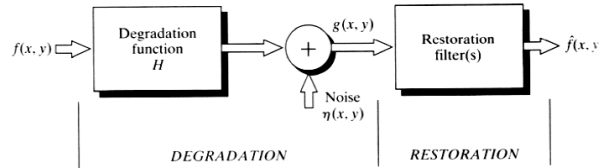


Figure 11 the model of degradation and restoration

3.2 Noise Models

Most of the noise degradation comes to digital images during their acquisition and/or transmission. A wide variety of factors may affect performance of imaging/transmission hardware. For instance, light levels and a sensor temperature of a CCD camera are two major factors determining the amount of noise in the resulting image. The spatial noise descriptor is the statistical behaviour of the intensity values in the noise component. Noise intensity can be considered as a random variable characterized by a certain PDF.

i. Gaussian Noise:

Gaussian noise is very attractive from a mathematical point of view since its DFT is another Gaussian process. PDF of Gaussian random variable is

$$p(z) = \frac{1}{\sqrt{2\pi}\sigma} e^{-\frac{(z-\bar{z})^2}{2\sigma^2}} \quad \dots 14$$

Here z represents intensity, \bar{z} is the mean (average) value of z and σ is its standard deviation. σ^2 is the variance of z . The PDF Curve of Gaussian noise is shown in figure 12.

ii. Rayleigh Noise:

Rayleigh noise is specified as

$$p(z) = \frac{2}{b}(z-a)e^{-\frac{(z-a)^2}{b}} \quad \text{For } z \geq a \quad \dots 15$$

The mean and variance are given by

$$\bar{z} = a + \sqrt{\pi b}/4 \quad \dots 16$$

$$\sigma^2 = \frac{b(4-\pi)}{4} \quad \dots 17$$

The Rayleigh density is useful for approximating skewed histograms. Used in range imaging. The PDF Curve of Rayleigh noise is shown in figure 12.

iii. Erlang (Gamma) Noise:

Erlang is specified as

$$p(z) = \frac{a^b z^{b-1}}{(b-1)!} e^{-az} \quad \text{For } z \geq 0 \quad \dots 18$$

Here $a > 0$ and b is a positive integer. The mean and variance are given by

$$\bar{z} = b/a \quad \dots 19$$

$$\sigma^2 = b/a^2 \quad \dots 20$$

When the denominator is the gamma function, the PDF describes the gamma distribution. The PDF Curve of Erlang noise is shown in figure 12.

iv. Exponential Noise:

Exponential noise is specified as

$$p(z) = ae^{-az} \quad \text{For } z \geq 0 \quad \dots 21$$

Here $a > 0$. The mean and variance are given by

$$\bar{z} = 1/a \quad \dots 22$$

$$\sigma^2 = 1/a^2 \quad \dots 23$$

Exponential PDF is a unique case of Erlang PDF with $b = 1$. Used in laser imaging. The PDF Curve of Exponential noise is shown in figure 12.

V. Uniform Noise:

Uniform noise is specified as

$$p(z) = \frac{1}{b-a} \quad \text{For } a \leq z \leq b \quad \dots 24$$

The mean and variance are given by

$$\bar{z} = \frac{a+b}{2} \quad \dots 25$$

$$\sigma^2 = \frac{(b-a)^2}{12} \quad \dots 26$$

The PDF Curve of Uniform noise is shown in figure 12.

vi. Impulse Noise:

Impulse noise (salt-and-pepper) is specified as

$$p(z) = \begin{cases} P_a \\ P_b \\ 0 \end{cases} \quad \dots 27$$

If $b > a$, intensity b will appear as a light dot on the image and appears as a dark dot frequently, if a and b are saturated values, resulting in positive impulses being white and negative impulses being black. This noise shows up when quick transitions – such as faulty switching – take place. The PDF Curve of Impulse noise is shown in figure 12.

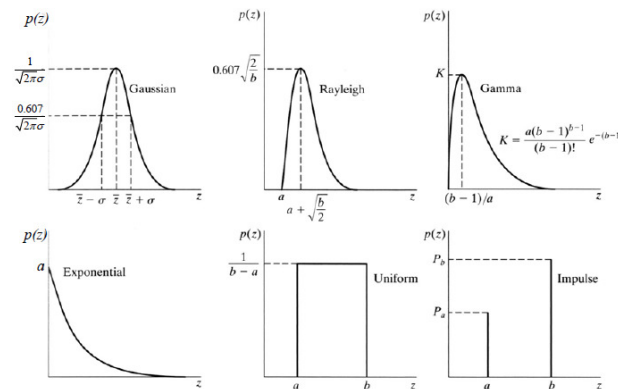


Figure 12 the Probability Density Functions of Different Noise Model

3.3 Spatial Domain Filtering Technique

i. Low Pass Filter (Smoothing Filter)

Smoothing filters are utilized for blurring and for noise reduction. Blurring is used in pre-processing steps, such as removal of small details from an image prior to (large) object extraction, and bridging of small gaps in lines or curves. Noise reduction can be accomplished by blurring with a linear filter and also by nonlinear filtering. The response of a smoothing, linear spatial filter is simply the average of the pixels include in the neighbourhood of the filter mask. These filters sometimes are called low pass filters.

By replacing the value of every pixel in an image by the average of the gray levels in the neighbourhood defined by the filter mask, this process results in an image with reduced “sharp” transitions in gray levels. Because random noise typically consists of sharp transitions in gray levels, the most obvious application of smoothing is noise reduction. However, edges also are characterized by sharp transitions in gray levels, so averaging filters have the undesirable side effect that they blur edges. Another application of this type of process includes the smoothing of false contours that result from using an inadequate number of gray levels. A major use of averaging filters is in the reduction of “irrelevant” detail in an image. Use of the first filter yields the standard average of the pixels in the mask. This can best be seen by substituting the coefficients of the mask into equation 28

$$R = \frac{1}{9} \sum_{i=1}^9 Z_i \quad \dots 28$$

Which is the average of the gray levels of the pixels in the 3×3 neighborhood defined by the mask. Note that, instead of being $1/9$, the coefficients of the filter are all 1's. The idea here is that it is computationally more efficient to have coefficients valued 1. At the end of the filtering process the entire image is divided by 9. A $m \times n$ mask would have a normalizing stable equal to $1/mn$. A spatial averaging filter in which all coefficients are equal is sometimes called a box filter.

ii. High Pass Filter (Sharpening Filter)

The principal objective of sharpening is to highlight fine detail in an image or to enhance detail that has been blurred, either in error or as a natural effect of a particular method of image acquisition.

Uses of image sharpening vary and include applications ranging from electronic printing and medical imaging to industrial inspection and independent guidance in martial systems. These filters sometimes are called high pass filters.

iii. Max Filter

The max filter plays a key role in low level image processing and vision. It is identical to the mathematical morphological operation: dilation. The brightest pixel gray level values are identified by this filter. It has been applied by many researchers to remove pepper noise. Though it removes the pepper noise it also removes the block pixel in the border. This filter has not yet applied to remove the speckle in medical image. Hence it is proposed for speckle noise removal from the medical image. It is expressed as:

$$f(x, y) = \max \{ g(s, t) \}, (s, t) \in S_{xy} \quad \dots 29$$

It reduces the intensity deviation between adjacent pixels. Implementation of this method for smoothing images is easy and also reducing the amount of intensity deviation between one pixel and the next. The result of this filter is the max selection processing in the sub image area S_{xy} .

iv. Min Filter

The min filter plays a significant role in image processing and vision. It recognizes the darkest pixels gray value and retains it by performing min operation. This filter was proposed for removing the salt noise from the image by researchers. Salt noise has very high values in images. The operation of this filter can be expressed as:

$$f(x, y) = \min_{(s,t) \in S_{xy}} \{ g(s, t) \} \quad \dots 30$$

It removes noise better than max filter but it removed some white points around the border of the region of the interest. In this filter each output pixel value can be calculated by selecting minimum gray level value of the chosen classical window.

V. Median Filter

It is so called as the median of all pixels in a local region of an image. It performs much better than arithmetic mean filter in removing salt and pepper noise from an image and in preserving the spatial details contained within the image. This method is particularly effective when the noise pattern consists of strong, spike like components and the characteristic to be preserved is edge sharpness.

Vi. Geometric Mean Filter

The gray level of pixel (x, y) in g , the Geometric filter replaces the gray level $f(x, y)$ by taking into account the surrounding detail and attenuating the noise by lowering the variance. This filter is known as smoothing spatial filters, with the median and geometric mean filters outperforming the arithmetic mean filter in reducing noise while preserving edge details. Increasing neighbourhood size, n , results in higher noise attenuation, but also loss of edge detail.

The geometric mean filter is member of a set of nonlinear mean filters, which are better at removing Gaussian type noise and preserving edge features than the arithmetic mean filter. The geometric mean filter is very susceptible to negative outliers. The geometric mean filter is defined as:

$$f(x, y) = \left[\prod_{(s,t) \in S_{xy}} g(s, t) \right]^{\frac{1}{mn}} \quad \dots 31$$

It is not suitable for removing impulse noise in the image each output pixel is given by the product of the pixels in the sub image window and raised to the power $1/mn$. Where m is number of rows in the image and n is number of columns in the image. It is better than mean filter in smoothing but it tends to lose less image detail in the process.

Geometric mean filter did not blur the image as much as mean filter. It is suitable for Gaussian noise. The output of each pixel is calculated by the power of reciprocal of the image size of the product of all pixels values in the classical window S_{xy} .

Vii Lee Filter

The Lee filter is based on a linear speckle noise model and a minimum mean square error (MMSE) design approach. The Lee filter identifies regions with low and constant variation as areas for noise reduction. In a region with no signal activity, the filter outputs the local mean. When signal activity is detected, the filter passes the original signal through unchanged. This is achieved by implementing a filter of the form specified by equation 32

$$\hat{R} = W I_t + (1 - W) \bar{I} \quad \dots 32$$

Where it is the central pixel in the I^{th} window and W is the weighting function range between 0 to 1 for regions with high signal act. The weighting function is calculated according to equation 33

$$W = 1 - \frac{C_u^2}{C_I^2} \quad \dots 33$$

Where $C_u = \frac{\sigma_u}{\bar{u}}$ and $C_I = \frac{\sigma_I}{\bar{I}}$ are the coefficient of variation of the noise is u and the image is I . In areas of high variance, edges are assumed and little to no noise smoothing is done.

In other words, the Lee filters smoothes away noise, but leaves fine details unchanged. Therefore, its major drawback is that it leaves noise in the vicinity of edges and lines.

$$\bar{I} = \frac{1}{N} \sum_{i=1}^N t_i, \quad \sigma_I^2 = \frac{1}{N-1} \sum_{i=1}^N (t_i - \bar{I})^2 \quad \dots 34$$

The mean and standard deviation are calculated from local regions in the image defined by smaller windows generally with dimensions $3 \times 3, 5 \times 5, 7 \times 7$ within each window, the local mean and variance are estimated according to equation 34

Viii Kaun Filter

In the Kuan Filter the multiplicative noise model is first transformed into a signal-dependent additive noise model. Then the MMSE criterion is then applied to this model. The resulting filter has the same form as the Lee filter but with a different weighting function as shown in equation 35.

$$W = \frac{1 - \frac{C_u^2}{C_I^2}}{1 + C_u^2} \quad \dots 35$$

The Kuan filter made no estimate to the original model. From this point of view, it can be considered to be better to the Lee filter. The Kuan filter can be derived directly by applying the MMSE criterion to the multiplicative model.

Ix Frost Filter

The Frost filter differs from the Lee and Kuan filters with respect that the scene reflectivity R is estimated by convolving the observed image with the impulse response of the coherent imaging method. The system's impulse response is calculated by minimizing the mean square error between the observed image and the scene reflectivity model, assumed to be an autoregressive process. The resulting filter after a few simplifications can be written as.

$$\hat{I}_t = \exp(-KC_I^2|t|) \quad \dots 36$$

Where K is a constant controlling the damping rate of the impulse response functions at the pixel to be filter. When the variation coefficient C_I^2 is small, the filter behaves like an LP filter smoothing out the speckles; when C_I^2 is large, it has a propensity to preserve the original observed image. To improve upon the frost filter, suggest dividing an image into areas belonging to single of three classes:

Homogeneous areas in which the speckles may be eliminated simply by applying an LP filter

Heterogeneous areas in which the speckles are to be reduced while preserving texture Areas containing isolated point targets, where the filter should preserve the observed value.

Areas are classifying base on the variation coefficients, C_u and C_I . Modified Frost filters using this classification.

$$M(t) = \exp(-K\text{func}(C_I(t_0))|t|) \quad \dots 37$$

Where $\text{func}(C_I(t_0))$ is a hyperbolic function of $C_I(t_0)$ defined as follows.

$$\text{func}(C_I) = \begin{cases} 0, & \text{for } C_I(t_0) < C_u \\ \frac{C_I(t_0) - C_u}{C_{\max} - C_I(t_0)}, & \text{for } C_u \leq C_I(t_0) \leq C_{\max} \\ \infty, & \text{for } C_I(t_0) > C_{\max} \end{cases} \quad \dots 38$$

A adapted Lee filter may also be derived in this method. Comparing the modified filters with the original, it can be seen that at the two extremes (i.e. the homogeneous area class and isolated point target class) the output is forced to be equivalent to the averaged value and the observed value with out of filtering, respectively.

X. Wiener Filtering

The inverse and pseudo-inverse filters remain sensitive to noise. In the existence of additive white noise, it does not work well. Wiener filter can overcome this limitation. Wiener filtering is a method of restoring images in the presence of blur as well as noise.

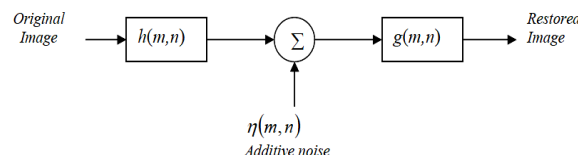


Figure 13 Process of Wiener Filtering

Wiener Filter is defined by

$$G(\omega_1, \omega_2) = \frac{H^*(\omega_1, \omega_2) S_{uu}(\omega_1, \omega_2)}{|H(\omega_1, \omega_2)|^2 S_{uu}(\omega_1, \omega_2) + S_{\eta\eta}(\omega_1, \omega_2)} \quad \dots 39$$

Where S_{uu} and $S_{\eta\eta}$ are Fourier transforms of the auto-correlation functions of $u(m,n)$ and $\eta(m,n)$ respectively.

Procedure:

- 1) Read an image (any size up to 512x512).
- 2) Calculate the three different $H(u,v)$ with $k=0.0025, 0.001$ and 0.00025 .
- 3) Calculate $G(u,v)$ with $H(u,v)$ obtained in 2), and show the three different blurred images.
- 4) Take the inverse filtering and Wiener filtering for each $G(u,v)$.
- 5) Show the restored images with ratios N/H , where N and H are power spectra of additive noise $\eta(m, n)$ and $h(m, n)$ respectively.

Xi Diffusion Filtering Technique

The diffusion filtering category includes filters based on anisotropic diffusion, coherence anisotropic diffusion and speckle-reducing anisotropic diffusion. These filters have been recently presented in the literature and are nonlinear filtering techniques. They simultaneously perform contrast enhancement and noise reduction by utilizing the coefficient of variation.

- Diffusion filter

Diffusion filters remove the noise from an image by modifying the image via solving a partial differential equation (PDE). Smoothing is carried out depending on the image edges and their directions. Anisotropic diffusion is an efficient nonlinear technique for concurrently performing contrast enhancement and noise reduction. It smoothes homogeneous image regions, but retains image edges without requiring any information from the image power spectrum. It may, thus, directly be applied to images.

Consider applying the isotropic diffusion equation given by

$$\frac{dg_{i,j,t}}{dt} = \text{div}(d\nabla g) \quad \dots 40$$

using the original noisy image $g_{i,j,t=0}$ as the initial condition, where $g_{i,j,t=0}$ is an image in the continuous domain, i and j specify the spatial position, t is an artificial time parameter, d is the diffusion constant, and ∇g is the image gradient. Modifying the image according to this linear isotropic diffusion equation is equivalent to filtering the image with a Gaussian filter.

- Anisotropic diffusion filtering

In anisotropic diffusion the main motto is to encourage smoothening within the region in preference to the smoothening across the edges.

Perona and Malik replaced the classical isotropic diffusion equation, as described above, by the introduction of a function $d_{i,j,t} = f(|\nabla g|)$ that smoothes the original image while trying to preserve brightness discontinuities with

$$\frac{dg_{i,j,t}}{dt} = \text{div}[d_{i,j,t} \nabla g_{i,j,t}] = \left[\frac{d}{d_i} d_{i,j,t} \frac{d}{d_i} g_{i,j,t} \right] + \left[\frac{d}{d_j} d_{i,j,t} \frac{d}{d_j} g_{i,j,t} \right] \quad \dots 41a$$

Where $|\nabla g|$ is the gradient magnitude, and $d(|\nabla g|)$ is an edge stopping function, which is chosen to satisfy $d \rightarrow 0$ when $|\nabla g| \rightarrow \infty$, so that the diffusion is stopped across edges.

This function, called the diffusion coefficient $d(|\nabla g|)$, which is a monotonically decreasing function of the gradient magnitude $|\nabla g|$, yields intraregion smoothing and not interregional smoothing by impeding the diffusion at image edges. It increases smoothing parallel to the edge and stops smoothing perpendicular to the edge, as the highest gradient values are perpendicular to the edge and dilated across edges. The choice of $d(|\nabla g|)$ can greatly affect the area to which discontinuities are preserved. For example, if $d(|\nabla g|)$ is constant at all locations, then smoothing progresses in an isotropic manner. If $d(|\nabla g|)$ is allowed to vary according to the local image gradient, then we have anisotropic diffusion.

A basic anisotropic PDE is given in Eq. (41a). Two different diffusion coefficients were proposed in Reference and also derived in Reference. The diffusion coefficients suggested were

$$d(|\nabla g|) = \frac{1}{1 + (|\nabla g_{i,j}|/K)^2} \quad \text{and} \quad cd(|\nabla g|) = \frac{2(|\nabla g_{i,j}|)}{2 + (|\nabla g_{i,j}|/K_1)^2} \quad \dots 41b$$

Where K and K_1 are positive gradient threshold parameters, known as diffusion or flow constants. The diffusion coefficient in Eq. (41b) was used as it was found to perform better in our images

A discrete formulation of the anisotropic diffusion in Eq. (41a) is

$$\frac{dg_{i,j}}{dt} = \frac{\lambda}{|\eta_s|} \{ d_{i+1,j,t} [g_{i+1,j} - g_{i,j}] + d_{i-1,j,t} [g_{i-1,j} - g_{i,j}] + d_{i,j+1,t} [g_{i,j+1} - g_{i,j}] + d_{i,j-1,t} [g_{i,j-1} - g_{i,j}] \} \quad \dots 42a$$

Where the new pixel gray value $g_{i,j}$ at location i, j is

$$f_{i,j} = g_{i,j} + \frac{1}{4} \frac{dg_{i,j}}{dt} \quad \dots 42b$$

Where $d_{i+1,j,t}$, $d_{i-1,j,t}$, $d_{i,j+1,t}$, and $d_{i,j-1,t}$ are the diffusion coefficients for the west, east, north, and south pixel directions, respectively, in a four-pixel neighbourhood around the pixel i, j where diffusion is computed. The diffusion coefficient leads to the largest diffusion where the nearest-neighbour difference is largest (the largest edge), whereas the smallest diffusion is calculated where the nearest neighbour difference is smallest (the weakest edge).

The constant $\lambda \in R^+$ is a scalar that determines the rate of diffusion, η_s represents the spatial neighbourhood of pixel i, j , and $|\eta_s|$ is the number of neighbors (generally four except at the image boundaries).

Perona and Malik linearly approximated the directional derivative in a particular direction as $\nabla g_{i,j} = g_{i+1,j} - g_{i,j}$ (for the east direction of the central pixel i, j). Modifying the image according to Eq. (42), which is a linear isotropic diffusion equation, is the similar like to filtering the image with a Gaussian filter.

- Anisotropic Diffusion Filter for Speckle-Reducing (ADSR)**

The essence of speckle-reducing anisotropic diffusion is the replacement of the gradient-based edge detector C_d ($|\nabla g|$) in an original anisotropic diffusion PDE with the instantaneous coefficient of variation that is suitable for speckle filtering C_{dsr} ($|\nabla g|$). The speckle-reducing anisotropic diffusion filter for de-speckle uses two seemingly different methods, namely, the Lee [3, 39, 83, 85] and Frost diffusion filters. A more general updated function for the output image by extending the PDE versions of the de-speckle filter is

$$f_{i,j} = g_{i,j} + \frac{1}{\eta_s} \text{div}(C_{iov}(|\nabla g|) \nabla g_{i,j}) \quad \dots 43$$

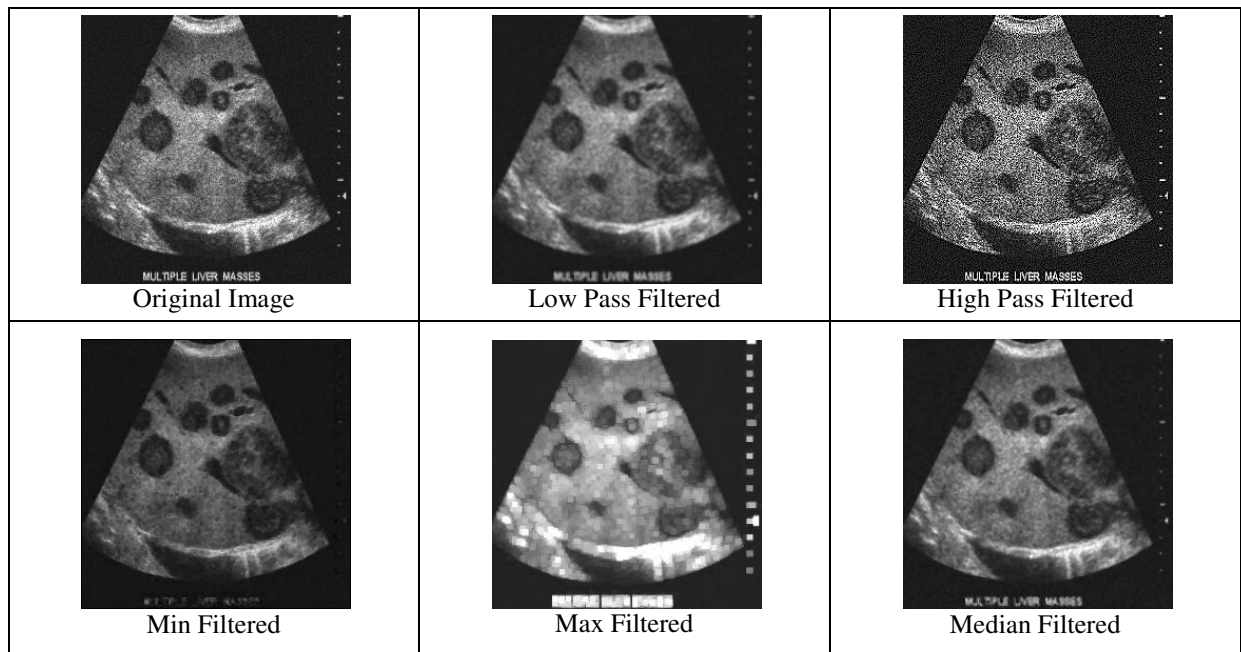
The diffusion coefficient for the speckle anisotropic diffusion C_{dsad} ($|\nabla g|$) is derived as

$$C_{iov}(|\nabla g|) = \frac{\frac{1}{2} |\nabla g_{i,j}|^2 - \frac{1}{16} (\nabla^2 g_{i,j})^2}{(g_{i,j} + \frac{1}{4} \nabla^2 g_{i,j})^2} \quad \dots 44$$

It is required that $C_{iov}(|\nabla g|) \geq 0$. The above instantaneous coefficient of variation combines a normalized gradient magnitude operator and a normalized Laplacian operator to act like an edge detector for speckle images. A high relative gradient magnitude and a low relative Laplacian indicate an edge. The Speckle-reducing anisotropic diffusion filter utilizes speckle-reducing anisotropic diffusion after Eq. (42) with the diffusion coefficient $C_{iov}(|\nabla g|)$ in Eq. (44).

3.4 Results of Different Restoration Technique

Results of Basic Filtering Techniques for Ultrasonography Images



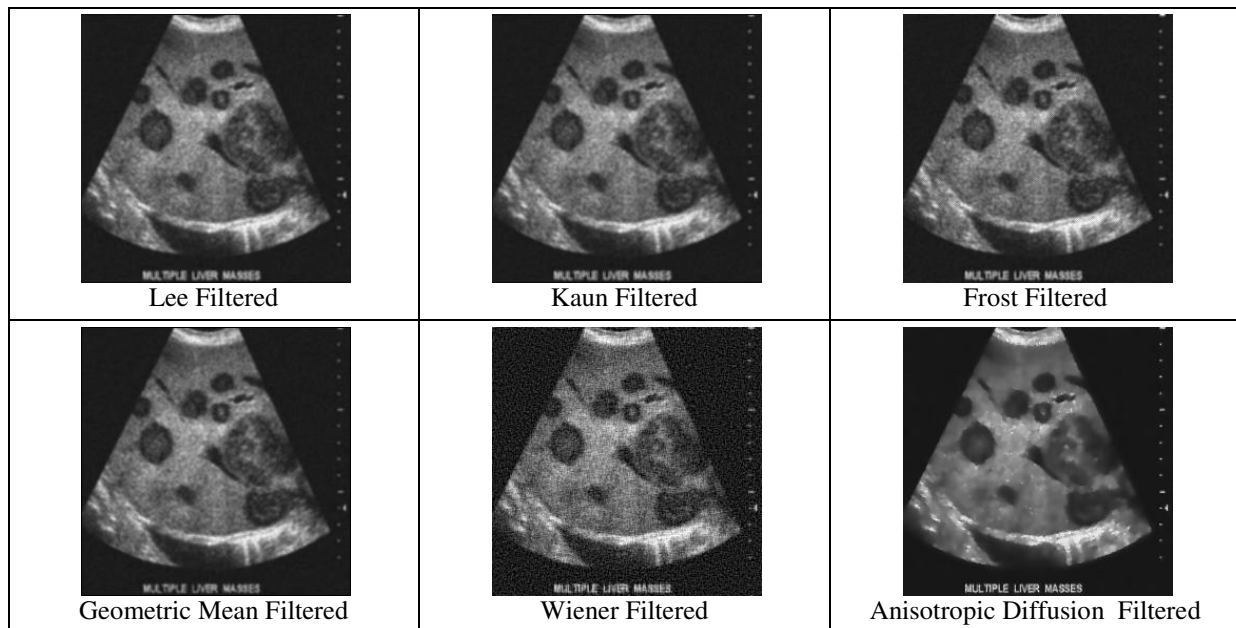


Figure 14 Results of basic filtering technique on USG Focal Liver Image.

TABLE 1 RESULTS OF QUALITY ASSESSMENT PARAMETERS FOR USG FOCAL LIVER IMAGE

SR.NO	FILTERING METHOD	MSE	PSNR	COC
	Noisy Image	135.0891	26.8246	0.9902
1	Low Pass Filter	86.2728	28.7721	0.9937
2	High Pass Filter	2.3972e+003	13338	0.8592
3	Min Filter	688.5606	19.7514	0.9810
4	Max Filter	2.0073e+003	15.1047	0.9671
5	Median Filter	103799	27.9446	0.9924
6	Lee Filter	95826	28.3727	0.9931
7	Kaun Filter	95826	28.3727	0.9931
8	Frost Filter	219.0612	27251	0.9841
9	Geometric Mean Filter	6.8000e+003	9.8057	0.9917
10	Wiener Filter	6.7984e+003	9.8067	0.9782
11	Anisotropic Diffusion	0.0013	77.1367	0.9945

Conclusion

In this paper, we introduce various techniques for restoration of Medical Ultrasound images it can be concluded that spatial domain filtering methods such as, lee, Kuan, frost, Anisotropic Diffusion Filter for Speckle Reduction (ADSR), Mean and Median filtering techniques and seen that speckle noise is difficult to reduce from the medical ultrasound image with spatial domain adaptive filter. Through the experiment on our ultrasound images results based on performance parameter and visualisation are shown in this paper. The experiment results prove that the PDE based Anisotropic Diffusion filter gives better noise reduction and the output images prove Anisotropic Diffusion filter the image with less information loss.

Bibliography

1. Rafael C. Gonzalez and Richard E. Woods, "Digital Image Processing", Prentice-Hall, Inc., 2002.
2. Huiyu, Jiahua Wu and jianguo Zhang, "Digital Image Processing Part-1", Ventus Publishing ApS, 2010.
3. Isaac N Bankman, "Handbook of Medical Imaging Processing and Analysis", Academic Press, A Harcourt Science and Technology Company 2000.
4. Jasjit S. Suri, David C. Wilson and Swami Laxminarayan, "Handbook of Biomedical Image Analysis" Kluwer Academic / Plenum Publishers, 2005.
5. Geoff Dougherty, "Digital Image Processing for Medical Applications", Cambridge Press, 2009.
6. William R. Hendee and E. Russell Ritenour, "Medical Imaging Physics", Wiley-Lis, Inc., 2002.
7. Atam P Dhawan, H K Huang and Dae-Shik Kim, "Principles And Advanced Methods In Medical Imaging And Image Analysis", World Scientific Publishing Co. Pte. Ltd. 2008.

8. Emanuele Neri Davide Caramella and Carlo Bartolozzi, "Image Processing in Radiology Current Applications", Springer-Verlag Berlin Heidelberg ,2008.
9. Vadim Kuperman, "Magnetic Resonance Imaging-Physical Principles and Applications", Academic Press, A Harcourt Science and Technology Company 2000.
10. Joseph V. Hajnal Derek L.G. Hill David J. Hawkes, "Medical Image Registration", CRC press, 2001.
11. Jiri-Jan, "Medical Image Processing Reconstruction and Restoration", Taylor & Francis Group, LLC, 2006.
12. Christos P. Loizou and Constantinos S. Pattichis, "Despeckle Filtering Algorithms and Software for Ultrasound Imaging", Morgan & Claypool, 2008.
13. Mohamed A. Mohamed, Fatma Abou-Chadi and Bassem K.Ouda, "Denoising Functional MRI: A Comparative Study of Different Temporal Techniques."
14. M. Sifuzzaman, M.R. Islam and M.Z. Ali, "Application of Wavelet Transform and its Advantages Compared to Fourier Transform" Journal of Physical Sciences, Vol. 13, 2009, 121-134.
15. K. Than gavel, R. Manalapan, and I. Laurence Aroquiaraj, "Removal of Speckle Noise from Ultrasound Medical Image based on Special Filters: Comparative Study, ICGST-GVIP Journal, ISSN 1687-398X, Volume (9), Issue (III), June 2009.
16. Yongjian yu and scoot t. Acton, senior member, IEEE, "speckle reducing anisotropic diffusion", IEEE transactions on image processing, vol. 11, no. 11, November 2002.
17. M. Mansourpour, M.A.Rajabi, and J.A.R. Blais," effects and performance of speckle noise reduction filters on active radar and SAR images, dept. of geometrics eng., university of Tehran, Tehran, 14395-515 Iran.
18. Venkata rukmini, "filter selection for speckle noise reduction", electronic instrumentation & control engineering to thapar university, patiala,
19. P. Perona and J. Malik, "Scale space and edge detection using anisotropic diffusion," *IEEE Trans. Pattern Anal. Machine Intell.*, vol.12, pp. 629–639, July 1990.
20. J.S. Lee, "Speckle analysis and smoothing of synthetic aperture radar images," *Comp. Graphics Image Process.*, vol. 17, pp. 24–32, 1981, doi: 10.1016/S0146-664X(81)80005-6.
21. Pavithra P, Ramyashree N, Shruthi T.V and Dr. Jharna Majumdar, "Image Enhancement by Histogram Specification Using Multiple Target Images," Special Issue of IJCCCT Vol.1 Issue 2, 3, 4; 2010 for International Conference [ACCTA-2010], 3-5 August 2010.
22. "Image processing Toolbox, User's Guide", The MathWorks, Inc.